The 15th International Symposium on Magnetic Bearings, August 3-6, 2016, Mojiko Hotel, Kitakyushu, Japan

ISMB15

Bias Flux Compensation in the 'Side-By-Side' Combination Radial/Axial Homopolar PM-Biased Active Magnetic Bearing

Alexei FILATOV, Larry HAWKINS and Chinmay UKIDVE
Calnetix Technologies
16323 Shoemaker Av., Cerritos, CA, 90703
E-mail: afilatov@calnetix.com

Abstract

'Side-By-Side' (SBS) Combination Radial/Axial Homopolar PM-Biased Active Magnetic Bearing design has been demonstrated to be an attractive solution for many applications requiring magnetic bearings. One of the key parts of this design is a bias flux compensation coil, which is needed to maintain a constant bias flux level under various axial loads and positions of the rotor. This is important, because variations in the bias flux in the SBS combo bearing affect operating parameters of both the radial and axial channels, including actuator gains and negative stiffnesses. Besides complicating the controls, changes of the bias flux may result in losses of the load capacities, which cannot be recovered thru improving the control algorithms.

Previously, the results of testing a standalone SBS combo bearing on a test rig have been presented. These included demonstrations of the effectiveness of the compensation for the effects of the axial control current on the overall bias flux. Those results showed good agreement with theoretical predictions, however, no analytical details of the compensation coil operation were given. The current paper presents the theoretical basis of the bias flux compensation. In addition, effects of the bias flux compensation on the properties of the magnetic suspension are demonstrated using a fully operational machine – a 200kW power range turbocompressor equipped with a SBS combination bearing.

Keywords : Active Magnetic Bearing, Combination Radial/Axial Magnetic Bearing, Permanent Magnet Bias, Homopolar Active Magnetic Bearing, Bias Flux Compensation, Actuator Design, Electromagnetic Analysis, Turbocompressor.

1. Introduction

'Side-By-Side' (SBS) Combination Radial/Axial Homopolar PM-Biased Active Magnetic Bearing design has been demonstrated to offer all the advantageous features of other active magnetic bearing technologies without suffering from their drawbacks (Filatov and Hawkins, 2014). Compared to the arrangements of separate axial and radial magnetic bearings, it benefits from a shorter axial length, lower part count, much lower aerodynamic drag and lower negative stiffness typical for combination bearings. On the other hand, compared to the other combination bearings, it features much better axial bandwidth typically demonstrated in arrangements of separate radial and axial bearings. Furthermore, for most machines, the "Side-By-Side" topology leads to the rotor construction that results in a higher first bending mode frequency than in the previous designs.

As a reminder, Fig. 1 illustrates the structure and operating principle of a SBS combination bearing previously described by Filatov (2013) and Filatov and Hawkins (2013). A similar design was disclosed earlier for example by Sortore et all., however, it was missing the bias compensation feature, which is the subject of this paper and which has been proven to be important for practical applications where the axial bearing length needs to be kept to the minimum.

Both radial and axial channels of the bearing utilize the same bias flux generated by a permanent magnet. When an axial control current is injected into the axial control coil, for example as shown in Fig. 1, it produces axial control magnetic flux. This control flux, in case of Fig.1, adds to the bias flux in the left axial air gap and subtracts from it in the right axial air gap. As a result, the net axial force F_{ax} develops that pulls the rotor to the left. Reversing the direction of

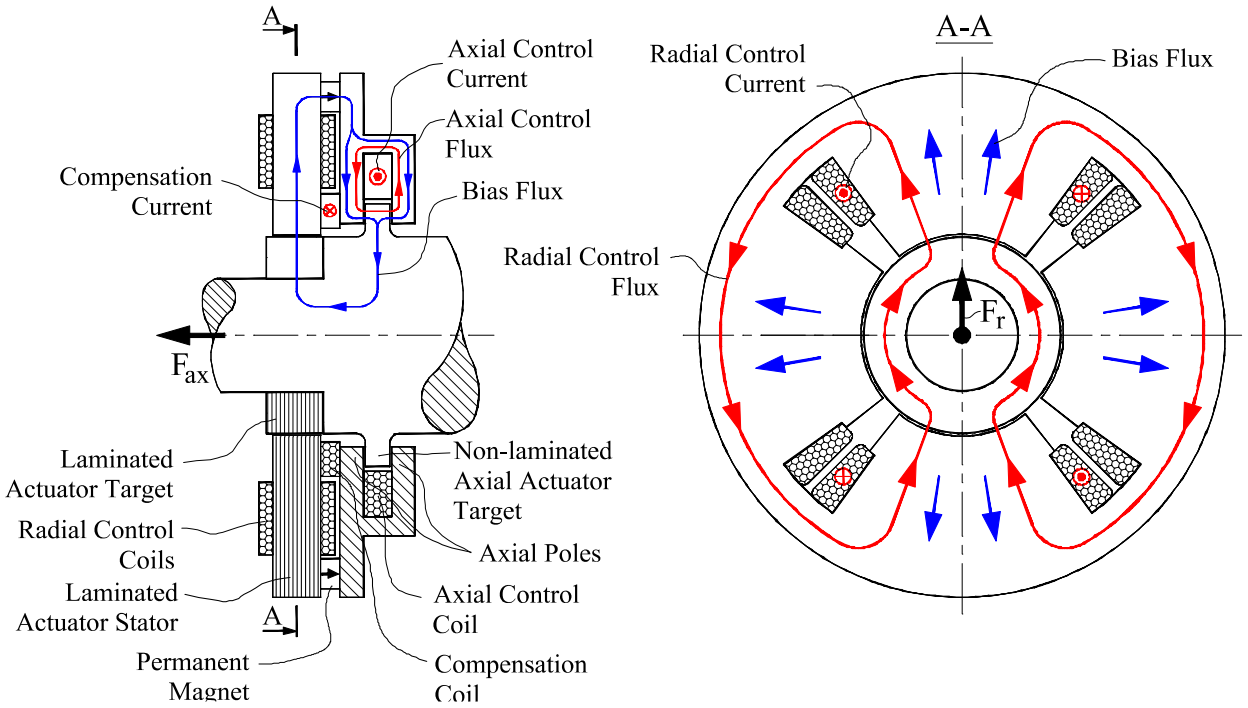

Fig. 1 Structure and operating principle of the SBS combination bearing.

the axial control current reverses the direction of the force F_{ax}.

Similarly, when two diametrically opposite radial control coils are energized with control currents, such as the two vertically oriented coils in Fig. 1, a radial control magnetic flux develops that overlaps with the bias flux. In the case shown in Fig. 1, the radial control flux adds to the bias flux in the upper radial air gap, but subtracts from it in the lower gap, resulting in the radial force F_r directed upwards.

The problem (and the need in the bias flux compensation) arises because in addition to the axial control flux path shown in Fig. 1, there also exists an alternative path for the magnetic flux induced by the axial control current, which leads to the existence of a leakage magnetic flux shown in Fig. 2. (From this point on we will refer to the control flux that would be produced in the absence of the leakage as the nominal control flux.) Note that the leakage flux in Fig. 2 is represented by two flux lines – a reason for this will become clear shortly.

Presence of the leakage magnetic flux has two negative consequences:

1. The radial bias flux changes with the axial control current and (to a lesser degree) with the axial position of the rotor resulting in the axial-to-radial cross-coupling. This is because the leakage flux in Fig. 2 adds to or subtracts from the bias flux shown in Fig. 1 in the radial air gaps and control poles.
2. The axial force-vs-current curve becomes non-linear because the control flux in the right axial pole is always greater in magnitude than the control flux in the left pole due to the added leakage flux.

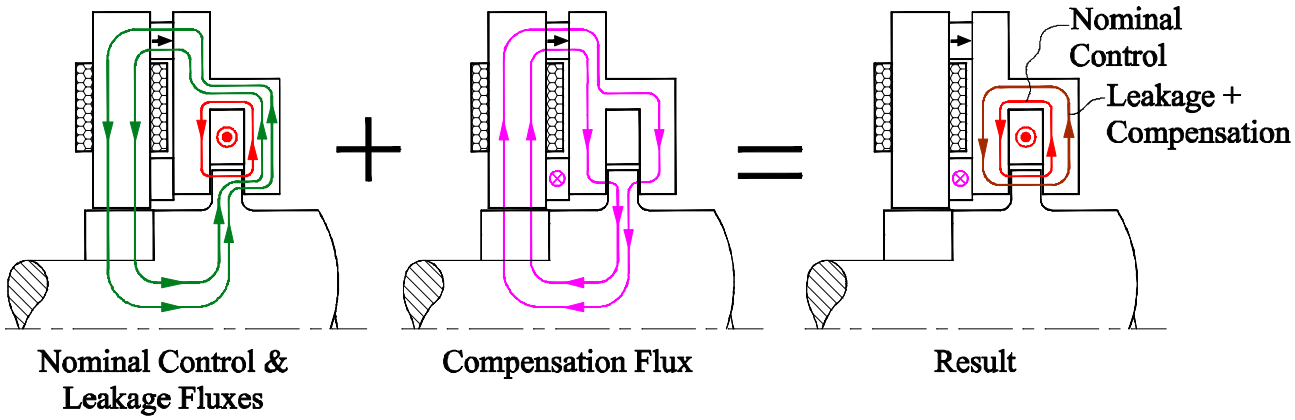

Fig. 2 Illustration of the bias compensation principle.

To overcome the effects of the leakage flux, a compensation coil is introduced that generates a compensation magnetic flux, which is also indicated by two flux lines in Fig. 2. In most part of the magnetic circuit the compensation flux flows along the same path as the leakage flux but in the opposite direction. The exception is the axial control circuit where the entire leakage flux flows thru the right pole, whereas the compensation flux splits: one line flows thru the left pole and one thru the right (this is why we used two flux lines to represent the leakage and the compensation fluxes).

One can see that in the most part of the magnetic circuit except for the two axial poles there are two leakage flux lines and two compensation flux lines going in the opposite directions, and, therefore, cancelling each other. In the right axial poles one compensation flux line directed radially inwards gets subtracted from two leakage flux lines going radially outwards, resulting in a single line of the net flux going outwards. In the left axial pole, where the leakage flux did not exist, there will be one line directed radially inwards introduced by the compensation flux. Thus, the results of the superposition of the leakage and compensation fluxes will look exactly as the axial control flux shown in Fig.1. With the right amount of compensation in place, there will be no changes of the radial bias flux and the net control fluxes in the left and the right poles will be the same (and slightly larger than the nominal control flux), as needed for the axial channel linearity.

In this paper we discuss analytical sizing of the compensation coil and present experimental results demonstrating effectiveness of the bias flux compensation using a fully operational turbocompressor on magnetic bearings as an example.

2. Sizing the compensation coil and defining compensation parameters

For accurate sizing the compensation coil and defining the compensation parameters (e.g. how the compensation current should change with the axial control current and the axial position of the rotor) an accurate analytical model of a SBS combination actuator is needed. Spatial distributions of quasi-static magnetic fields in the air space adjacent to soft-magnetic components are often estimated by dividing that air space into elementary shapes spanning from one magnetically equipotential surface to another. Magnetic reluctances of such elementary shapes are tabulated, and an equivalent electrical circuit can be built to calculate magnetic fluxes with those reluctances represented by equivalent resistances, permanent magnets represented by electrical batteries (including internal resistances) and coils with currents represented by lossless voltage sources (see, for example, McCaig, 1977) .

Figure 3 illustrates how the air space adjacent to the components of the SBS combo can be divided into elementary shapes. (Three axial cross-sections are used to show separately otherwise overlapping shapes.) Note that reluctances R_{rad}, R_{fr_rad}, $R_{leak\_ax\text{-}rad1}$, $R_{leak\_ax\text{-}rad2}$, R_{leak_rad1} and R_{leak_rad2} represent reluctances associated with individual radial poles (as illustrated in Fig. 3 for R_{rad} and R_{fr_rad}) and there are four radial poles in total.

Figure 4a shows a simplified equivalent schematic of the magnetic system per Fig. 3. Some of the magnetic reluctances shown in Fig. 3 are combined together in Fig. 4a as follows:

$R_{leak\_top} = R_{leak\_top1} \,||\, R_{leak\_top2} \,||\, R_{leak\_top3}$;

$R_{leak\_ax\text{-}rad} = R_{leak\_ax\text{-}rad1} \,||\, R_{leak\_ax\text{-}rad2}/4$ (divided by four because there are four poles with associated reluctances connected in parallel);

$R_{rad\_tot} = (R_{rad} \,||\, R_{fr\_rad} \,||\, R_{leak\_rad1})/4$;

$R_{ax1\_tot} = R_{ax1} \,||\, R_{fr\_ax1} \,||\, R_{leak\_ax1\text{-}shaft} \,||\, R_{leak\_ax1\text{-}trg\_top} \,||\, R_{leak\_ax1\text{-}trg\_btm}$; (1.1)

$R_{ax2\_tot} = R_{ax2} \,||\, R_{fr\_ax2} \,||\, R_{leak\_ax2\text{-}shaft} \,||\, R_{leak\_ax2\text{-}trg\_top} \,||\, R_{leak\_ax2\text{-}trg\_btm} \,||\, R_{fr\_ax2\text{-}shaft} \,||\, R_{leak\_ax2\text{-}shaft\_side}$; (1.2)

where symbol || means parallel connection, for example

$$a||b||c = \left\{\frac{1}{a}+\frac{1}{b}+\frac{1}{c}\right\}^{-1}.$$

Since parameters NI_{pm}, R_{pm} and two reluctances R_{leak_top} and $R_{leak\_ax\text{-}rad}$ connected in parallel with the permanent magnet do not change when the axial control current I_{ax} changes, for the total bias flux injected into the system Φ_{tot} to stay constant, the MMF drop across the permanent magnet U_{pm} must remain constant for given Φ_{tot} regardless of I_{ax}. This MMF is controlled by the main circuit branch connected in parallel with the magnet that carries the total bias flux Φ_{tot} and includes NI_{ax} and NI_{comp}. The equivalent electrical schematic for this branch is shown in Fig. 4b, with the magnet, along with two reluctances R_{leak_top} and $R_{leak\_ax\text{-}rad}$ connected in parallel with it being replaced by the terminal voltage U_{pm}. To calculate U_{pm} for a given Φ_{tot} we use Kirchoff's equations (2.1)-(2.5) below. Current loops and nodes corresponding

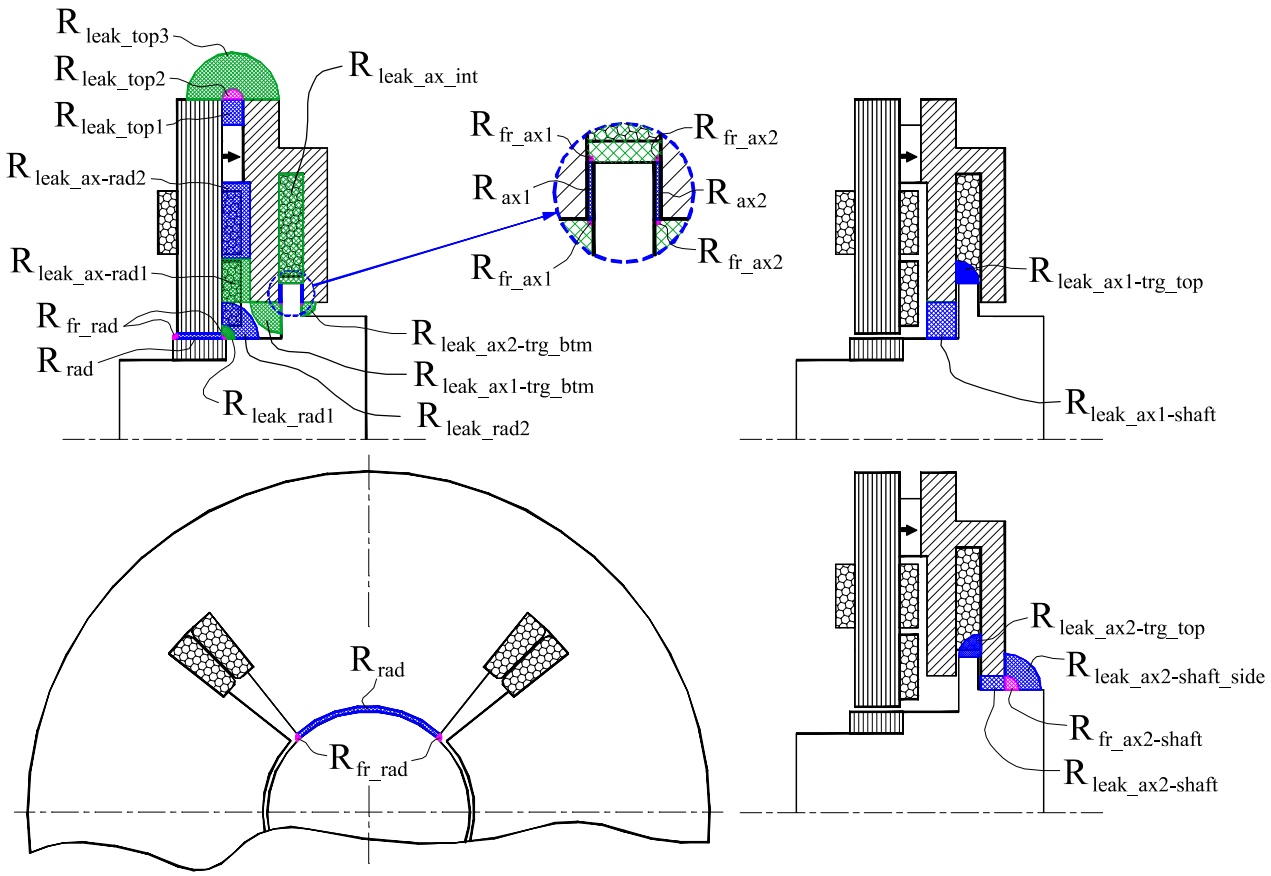

Fig. 3 Lumped magnetostatic model of a SBS combination bearing.

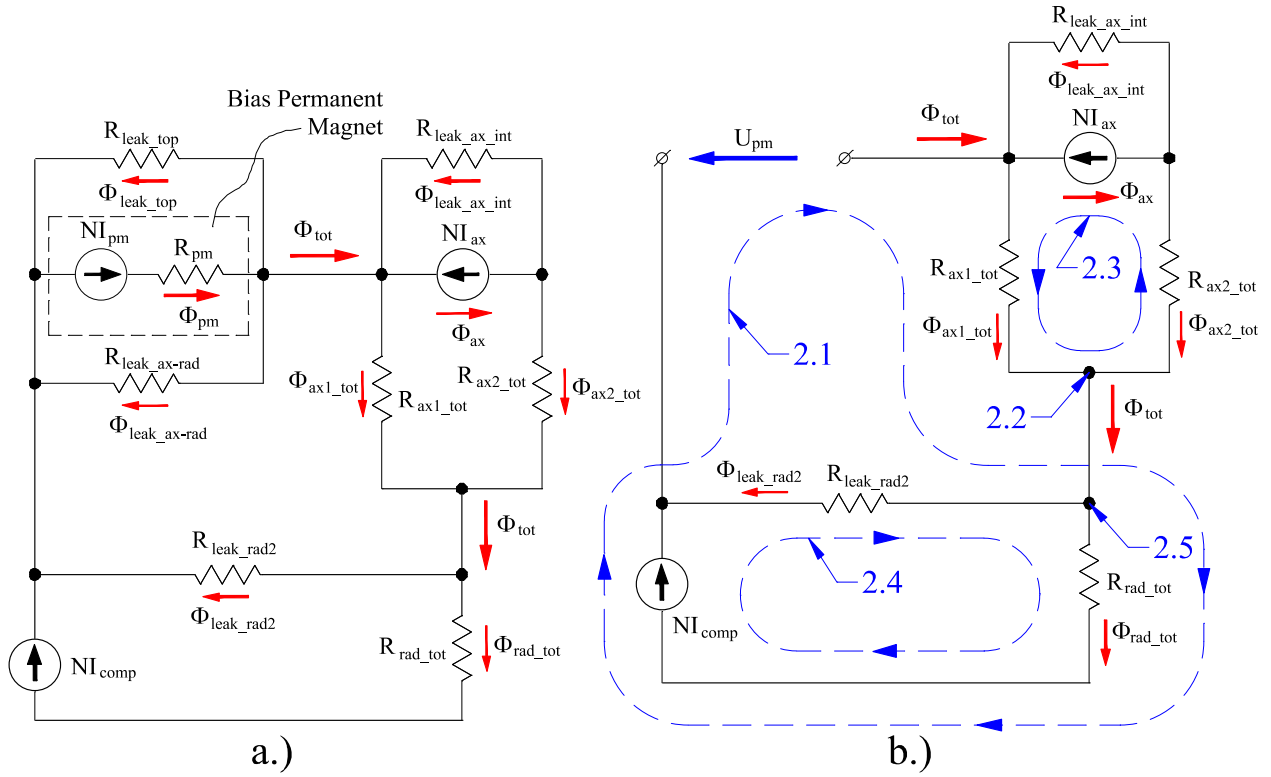

Fig. 4 Equivalent electrical schematics for the entire magnetic system (a) and its main bias flux branch (b).

to these Kirchoff's equations are shown on Fig. 4b for convenience and labeled with the corresponding numbers.

$$NI_{comp} + U_{pm} = \Phi_{ax1\_tot} \cdot R_{ax1\_tot} + \Phi_{rad\_tot} \cdot R_{rad\_tot} \quad (2.1)$$

$$\Phi_{tot} = \Phi_{ax1\_tot} + \Phi_{ax2\_tot} \quad (2.2)$$

$$NI_{ax} = \Phi_{ax1\_tot} \cdot R_{ax1_{tot}} - \Phi_{ax2\_tot} \cdot R_{ax2_{tot}} \quad (2.3)$$

$$\Phi_{tot} = \Phi_{rad\_tot} + \Phi_{leak\_rad2} \quad (2.4)$$

$$NI_{comp} = \Phi_{rad\_tot} \cdot R_{rad\_tot} - \Phi_{leak\_rad2} \cdot R_{leak\_rad2} \quad (2.5)$$

Using Eqs. (2.1) thru (2.5), the following link between U_{pm}, Φ_{tot}, NI_{ax} and NI_{comp} can be established:

$$U_{pm} = \Phi_{tot} \cdot \left(\frac{R_{ax2\_tot} \cdot R_{ax1\_tot}}{R_{ax2\_tot}+R_{ax1\_tot}} + \frac{R_{leak\_rad2} \cdot R_{rad}}{R_{leak\_rad2}+R_{rad}}\right) + NI_{ax}\left(\frac{R_{ax1\_tot}}{R_{ax1\_tot}+R_{ax2\_tot}}\right) - NI_{comp}\left(\frac{R_{leak\_rad2}}{R_{rad}+R_{leak\_rad2}}\right) \quad (3)$$

One can note that if

$$NI_{comp}\frac{R_{leak\_rad2}}{R_{rad}+R_{leak\_rad2}} = NI_{ax}\frac{R_{ax1\_tot}}{R_{ax1\_tot}+R_{ax2\_tot}},$$

then U_{pm} will be a function of Φ_{tot} only and will remain the same for any level of NI_{ax}.

Therefore, if the rotor position does not change and we set the compensation current to be a linear function of the control current so that

$$NI_{comp} = NI_{ax}\frac{R_{ax1\_tot}}{R_{ax1\_tot}+R_{ax2\_tot}}\frac{R_{rad}+R_{leak\_rad2}}{R_{leak\_rad2}}, \quad (4)$$

then the operation point of the permanent bias magnet, and consequently, the total bias flux as well as the axial and the radial bias fluxes both will be independent of the axial control current.

In practice, R_{leak_rad2} is typically much larger than R_{rad}, and Eq. (4) can be reduced to

$$NI_{comp} = NI_{ax}\frac{R_{ax1\_tot}}{R_{ax1\_tot}+R_{ax2\_tot}} \quad (5)$$

The condition $R_{leak\_rad2} >> R_{rad}$ is even more easy to justify if we note that not the entire magnetic flux flowing thru the reluctance R_{leak_rad2} in Fig.3 is linked to the compensation coil contrary to a conservative assumption that is used in the equivalent electrical schematics shown in Figs. 4a and 4b.

It is important to keep in mind that both R_{ax1} and R_{ax2} are functions of the rotor axial position z, and, therefore, in general the compensation current I_{comp} should be a function of both the axial control current I_{ax} and the axial rotor position z.

Let's consider three practically important scenarios that provide more insights into the physics behind the Eq. (5) as well as some ideas on possible values of the compensation magnetomotive force.

1. $R_{ax1\_tot}=0$ (The rotor in Figs. 1 thru 3 is all the way to the left and the left axial air gap is closed). Equation (5) gives us $NI_{comp}=0$. Indeed, looking at Fig. 2 for example it is clear that when the actuator target is in contact with the left axial pole, this pole shunts the alternative leakage path for the magnetic flux induced by the axial control current thru radial poles and the bias magnet – the entire flux produced by the control current will be the proper control flux, there will be no leakage and no compensation needed.
2. $R_{ax2\_tot}=0$ (The rotor in Figs. 1 thru 3 is all the way to the right and the right axial air gap is closed). Equation (5) gives us $NI_{comp}=NI_{ax}$. In this case no compensation or bias flux would go thru the inner axial pole because of zero reluctance of the parallel path thru the outer axial pole: the bias flux, the leakage flux and the compensation flux will all follow the same path shown in Fig. 2 for the leakage flux. Apparently to eliminate the leakage flux in this case the net MMF from the sources encircled by the leakage flux loop has to be zero, i.e. $NI_{comp}=NI_{ax}$ (we selected opposite directions for the positive current flow in the compensation and the control coils at the beginning, this is why there is no minus sign here).
3. $R_{ax1\_tot}=R_{ax2\_tot}$ (If the axial poles and the adjacent portions of the rotor are perfectly symmetric with respect to the middle plane of the axial target, this condition would realize with the axial target in the centered position, i.e. left axial air gap is equal to the right axial air gap.) In this case Eq. (5) gives us $NI_{comp}=NI_{ax}/2$. This is normally a good first approximation for the compensation magnetomotive force, however, more often than not $R_{ax1\_tot} \neq R_{ax2\_tot}$ when the axial actuator target is centered. For example Fig. 3 shows a higher shaft diameter

under the right pole than under the left pole, which will lead to more magnetic flux leaking into the shaft from the right pole than from the left, and, consequently, $R_{ax1\_tot}>R_{ax2\_tot}$ at the centered position (R_{ax1_tot} and R_{ax2_tot} both include leakage fluxes).

The equations 4 and 5 are easier to interpret if we redraw and simplify the equivalent electrical schematic shown in Fig.4b as shown in Fig. 5a for $NI_{ax}=0$ and $NI_{comp}=0$, Fig. 5b for $NI_{ax}\neq 0$ and $NI_{comp}\neq 0$ and Fig. 5c for $R_{rad\_tot}<<R_{leak\_rad2}$.

The goal of the bias flux compensation is to ensure that the MMF drop across the magnet U_{pm} in cases shown in Figs 5b and 5c when $NI_{ax}\neq 0$ is the same as in Fig. 5a when $NI_{ax}=0$. To find an increase of the voltage U_{ax} in Fig. 5b compared to Fig. 5a we can assume $\Phi_{tot}=0$ and find from the contour 2.3:

$$\Delta U_{ax} = NI_{ax}\frac{R_{ax1\_tot}}{R_{ax1\_tot}+R_{ax2\_tot}}$$

Similarly, from the contour 2.4 we find:

$$\Delta U_{rad} = -NI_{comp}\frac{R_{leak\_rad2}}{R_{leak\_rad2}+R_{rad\_tot}}$$

For the total voltage U_{pm} in Fig. 5b to remain the same as in Fig. 5a, we need $\Delta U_{ax}+\Delta U_{rad}=0$ or

$$NI_{ax}\frac{R_{ax1\_tot}}{R_{ax1\_tot}+R_{ax2\_tot}} - NI_{comp}\frac{R_{leak\_rad2}}{R_{leak\_rad2}+R_{rad\_tot}} = 0,$$

which is our Eq. (4).

In case of $R_{rad\_tot}<<R_{leak\_rad2}$, similar analysis of Fig. 5c quickly leads to Eq. (5).

Since the values of the elementary reluctances associated with the axial poles are known functions of their dimensions, one can calculate their values as functions of the axial position of the rotor, and, consequently, the amount of the compensation magnetomotive force needed to maintain the constant bias flux as a function of the axial rotor position and the axial control current. A more accurate approach would be to calculate the compensation magnetomotive force dependence on the axial rotor position with FEA for a given current and then scale it linearly with the current since the dependence on the current would be linear (assuming no magnetic saturation).

3. Experimental demonstration of the effectiveness of the bias compensation

Previously we have demonstrated the validity of the bias flux compensation principle using a standalone SBS combination actuator mounted on a test rig (Filatov and Hawkins, 2013). In this paper we present some results of applying this principle to a fully operational turbocompressor. A schematic layout of the turbocompressor along with the axial loading fixture is shown in Fig. 6. The bias compensation coil was energized with a dedicated amplifier – a flexible

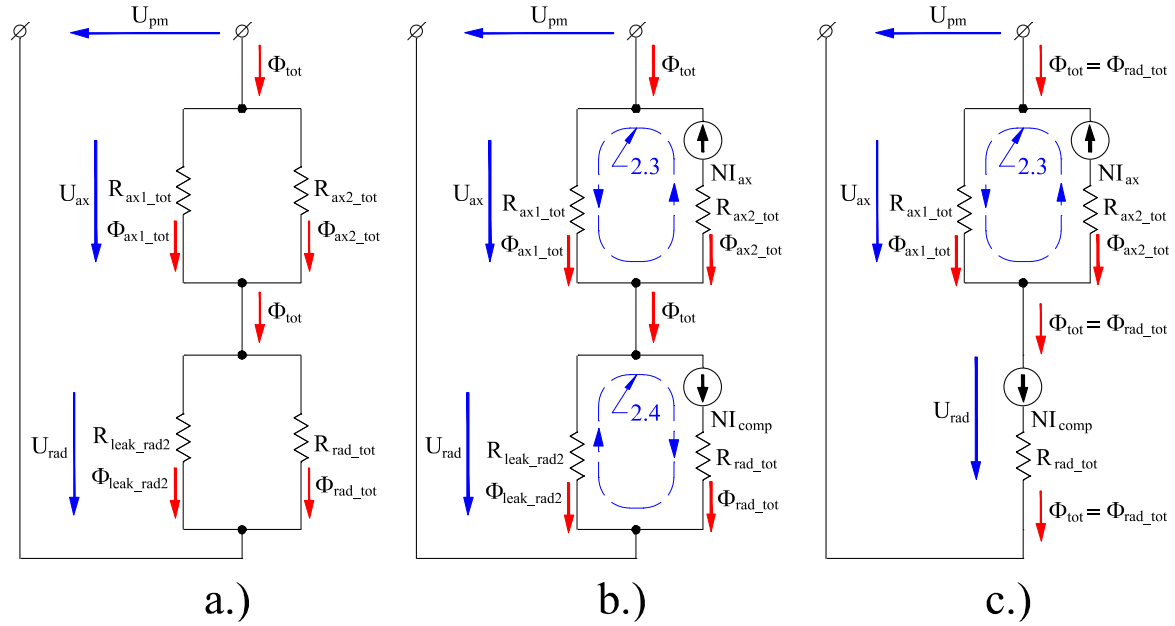

Fig. 5 Alternative and simplified representations of the branch electrical schematic shown in Fig. 4b.

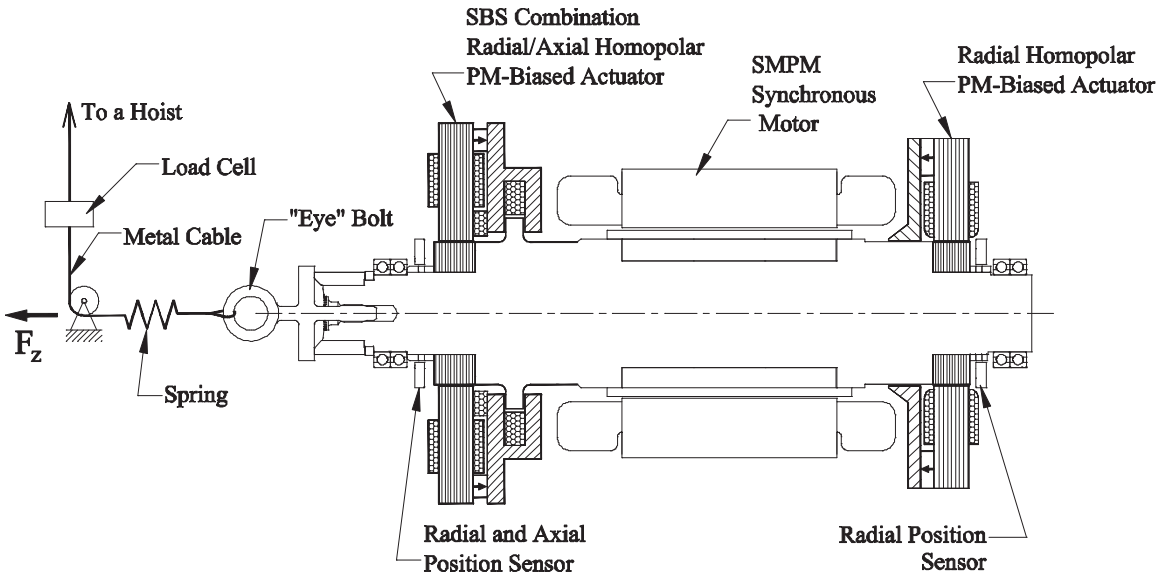

Fig. 6 Schematic layout of the turbocompressor used to demonstrate effectiveness of the bias flux compensation and axial loading arrangement.

approach that, in principle, allows compensation for a variety of factors affecting the bias flux including axial control current, axial rotor position, temperature, etc. In this paper, however, we'll focus on the axial control current only.

Figure 7 shows the results of the axial loading tests with and without the compensation as well as the compensation applied with the wrong current polarity. Theoretical predictions with and without the compensation are shown as well. It is to be noticed that two axial poles of the actuator in this machine had very different leakage reluctances associated with them, in part because the shaft OD was larger under the axial pole #2 than under the axial pole #1, similar to Fig.3. Since the amount of compensation needed to maintain Φ_{tot} and, therefore, the radial bias flux given by Eqs. (4) or (5) depends on the total axial pole reluctances (including leakages), whereas the leakage fluxes bypassing the axial air gaps do not contribute to the axial forces, finding the amount of compensation that would result in a fully symmetric (and linear) axial loading curve and a radial bias flux independent of the axial control current is not possible in asymmetric cases like this. As can be learned from Fig. 7, the amount of compensation chosen in this design is excessive from the perspective of optimizing the axial load curve, which shape changes from convex without the compensation to concave with the

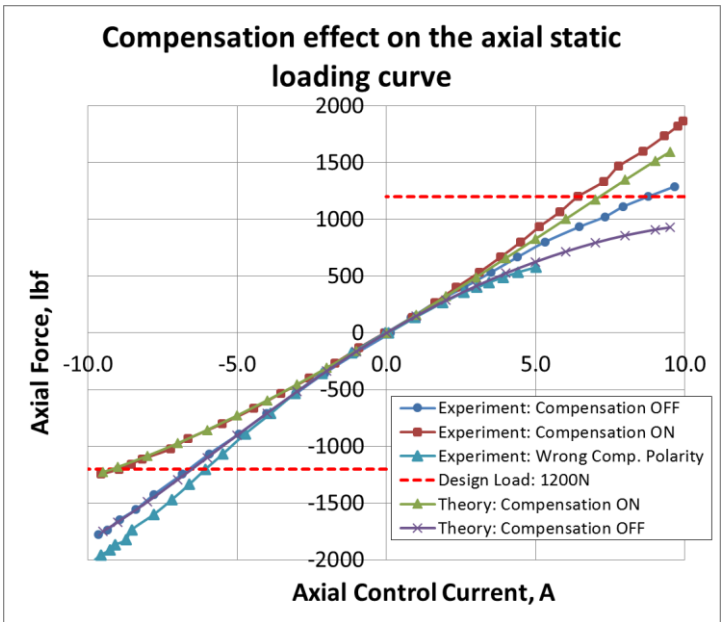

Fig. 7 Bias compensation effect on the axial static loading characteristic of a SBS combination bearing.

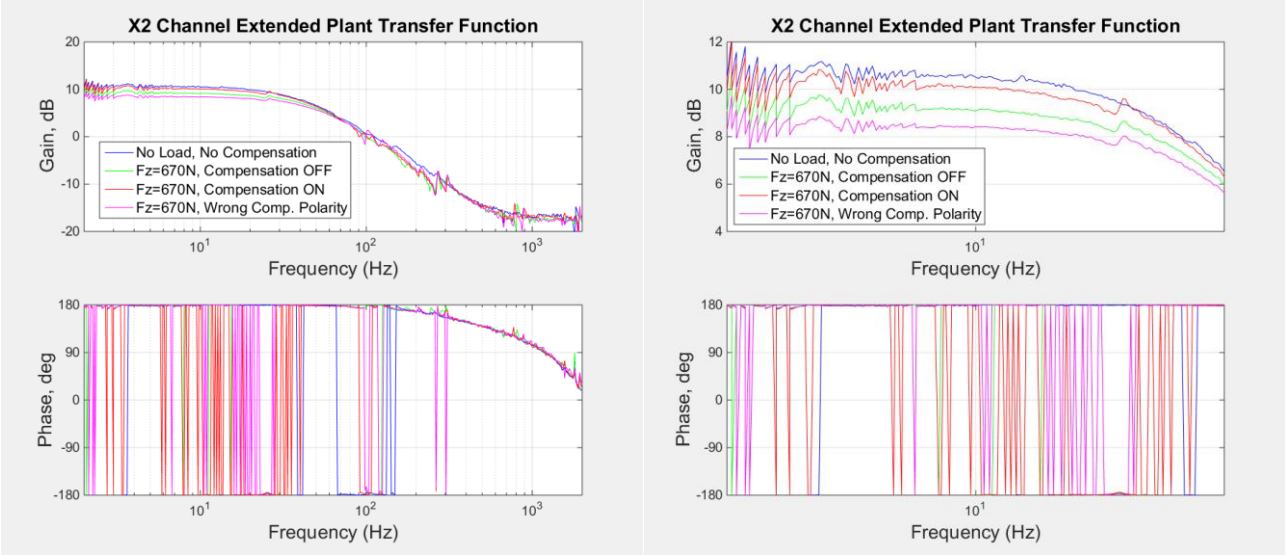

a.) b.)

Fig. 8 Measured radial plant transfer functions. a.) – the entire measurement frequency span; b – low frequency range.

compensation, skipping thru the linear shape somewhere in between. However, as shown below, the compensation chosen is still slightly less than the amount needed to fully eliminate the radial bias flux dependence on the axial control current.

Figure 8 shows radial plant transfer functions measured without axial load (as a benchmark) and then measured with 670N axial load applied (to induce the axial current) and the compensation being turned off, turned on, and applied with the wrong current polarity. Note that the amplitudes of the plant transfer functions are proportional to *Kr/Ki* (where *Kr* is the radial negative stiffness and *Ki* is the actuator gain) rather than *Kr* or *Ki* themselves. Nevertheless, the effect of the compensation on the radial transfer functions is very noticeable, especially in the low frequency range. As mentioned earlier, the level of compensation in this machine was not sufficient to completely overcome the radial bias flux dependence on the axial current, but larger level of compensation would lead to the axial actuator not meeting the static load capacity requirement in the negative direction (see Fig. 7). In other words, the level of compensation was a trade-off between maintaining a constant radial bias flux and fully utilizing the axial load capacity of the actuator in both directions.

5. Conclusions

The presented analytical model of the SBS combination radial/axial active magnetic bearing allows calculation of the bias compensation magnetomotive force needed to avoid bias flux dependence on the axial control current and, to a lesser degree, on the axial position of the rotor. The model also provides a deeper insight into the compensation mechanism disclosed in the previous publications.

Experimental data obtained on a fully functional turbocompressor equipped with a SBS combination bearing demonstrates the effectiveness of the bias compensation in both maintaining the constant radial bias flux as well as shaping the axial static loading curve.

References

Filatov A. and Hawkins L., Comparative Study of Axial/Radial Magnetic Bearing Arrangements for Turbocompressor Applications, Proceedings of ISMB14 (2014).

Filatov A., Electromagnetic Actuator, US Patent 8,482,174 B2 (2013).

Filatov A. and Hawkins L., Novel Combination Radial/Axial Homopolar Active Magnetic Bearing, Proceedings of the 1st Brazilian Workshop on Magnetic Bearings (2013).

McCaig, M., Permanent Magnets in Theory and Practice (1977), Pentech Press, London: Plymouth.

Sortore C. K., et all., Design of Permanent Magnet Biased Magnetic Bearings for a Flexible Rotor (1990), ROMAC conference, Charlottesville, VA, USA.